Modeling the electrochemical conversion of carbon dioxide to formic acid or formate at elevated pressures

Morrison, Andrew R.T.; van Beusekom, Vincent; Ramdin, Mahinder; Van den Broeke, Leo; Vlugt, Thijs J.H.; de Jong, Wiebren

DOI
10.1149/2.0121904jes

Publication date
2019

Document Version
Final published version

Published in
Journal of the Electrochemical Society

Modeling the Electrochemical Conversion of Carbon Dioxide to Formic Acid or Formate at Elevated Pressures

Andrew R. T. Morrison,[1] Vincent van Beusekom,[1] Mahinder Ramdin,[2] Leo J. P. van den Broeke,[2] Thijs J. H. Vlugt,[2] and Wiebren de Jong[1,z]

[1]*Large-Scale Energy Storage, Process & Energy Department, Faculty of Mechanical, Maritime and Materials Engineering, Delft University of Technology, 2628 CB Delft, The Netherlands*
[2]*Engineering Thermodynamics, Process & Energy Department, Faculty of Mechanical, Maritime and Materials Engineering, Delft University of Technology, 2628 CB Delft, The Netherlands*

In this work a model of an elevated pressure CO_2 electrolyzer producing primarily formate or formic acid is presented. It consists of three parts: a model of the bulk electrolyte, the diffusion layer, and the electrode surface. Data from the literature was used to validate both the bulk portion of the model, as well as the overall model. Results from the literature were further explored and explained by reference to the model and faradaic efficiency is predicted very well (R-Square of 0.99 for the fitted data, and 0.98 for the non-fitted data). The primary effect of increasing the pressure on a CO_2 electrolyzer is seen to be increasing the maximum attainable partial current density, while the faradaic efficiency and specific energy of formation plateau at pressures above 10–20 bar, at 95% and of 3.7 kWh/kg, respectively. Unlike the efficiencies, the profitability of running a reactor increases with pressure, following a similar trend as partial current density, showing the importance of this quantity as a performance metric of a CO_2 electrolyzer. In general this work shows the utility of a model of this sort in the design, evaluation and operation of CO_2 electrolyzers.
 [DOI: 10.1149/2.0121904jes]

Manuscript submitted November 27, 2018; revised manuscript received January 21, 2019. Published February 12, 2019.

Carbon dioxide in the atmosphere is well known to be a dire issue facing the planet. Finding ways to reduce CO_2 production, or even remove it from the atmosphere, is of high importance. According to the latest IPCC report a range of far-reaching measures would be required across all sectors of society. One of the proposed measures has to do with the reduction of CO_2 emissions from industry, and:

> *. . . such reductions can be achieved through combinations of new and existing technologies and practices, including electrification, hydrogen, sustainable bio-based feedstocks, product substitution, and carbon capture, utilization and storage (CCUS).*
>
> (IPCC report, Summary for policy makers, section C2.3, October 2018).[1]

With respect to large-scale CCUS applications related the conversion of CO_2 to C1 or C2 chemicals (chemicals containing one or two carbons, respectively) two main pathways can be envisaged. The first pathway is the conversion of CO_2 based on hydrogenation reactions, the second is the electrochemical conversion of CO_2 with water. In order to develop carbon dioxide utilization pathways a number of constraints need to be taken into account. First of all, renewable carbon from biomass or regenerative carbon from recycling of CO_2 should be the starting point for the future development of sustainable process routes for the synthesis of C1 and C2 chemical building blocks.[2] Second, for the hydrogenation routes, the hydrogen should be produced from renewable power and water electrolysis.[3–6]

With respect to the development of future production routes and CCU (carbon capture and utilization) applications a number of options are available. Either novel and emerging process routes need to be developed, or the captured CO_2 from the flue gas of existing production plants, like urea and methanol production, needs to be used/recycled in the existing operation.[7–10] A number of commercial processes have been realized on the second CO_2 utilization option. Mitsubishi Heavy Industries has deployed over 10 commercial CO_2 capture plants with a capture capacity from 200 to 500 ton CO_2 per day (tpd). Most of these plants capture the CO_2 from the flues of natural gas-fired turbines. The captured CO_2 is then used to enhance the existing production in an economically feasible way (with a pay-back period of 1 to 2 years).[11,12] In terms of novel and emerging process routes, a range of options are being developed that are broadly classified as power-to-chemicals (P2C), power-to-gas (P2G), or biomass-to-liquid (BtL) routes.[13–17] CO_2-based chemicals will be developed through a limited number of pathways which basically extend the current natural gas-based routes. More specifically, this will build on 1) the current natural gas to syngas to Fischer Tropsch liquids processes, or 2) routes based on methanol, like natural gas to and methanol to olefins (mainly ethylene and propylene) or methanol to gasoline.[16–19] Another emerging process route that is more removed from the traditional routes is the concept of the formate bio-economy, where formic acid or formate ($HCOO^-$) is used as a syngas (mixture of CO and H_2) equivalent for the production of a range of chemicals.[20] Other cases use formic acid as a source of hydrogen, or more practically, as a source of carbon monoxide (CO).[21,22]

The formate or formic acid in the formate bio-economy route would be from CO_2 electrolyzers, which are the focus of this work. In these electrochemical reactors the cathodic half-reaction is the CO_2 reduction reaction and the anodic half-reaction is the oxygen evolution reaction. CO_2 reduction has several possible products (e.g. formic acid, carbon monoxide, formaldehyde, ethylene, oxalate and more) depending on several process conditions of the reactor. For example the potential, flow rate, pressure, electrolyte (aqueous or non-aqueous, which salts, etc.) all influence the selectivity. In particular it is thought that high CO_2 pressure, low temperature and targeting the two-electron products will minimize energy consumption.[23,24] Recent developments in the field of electrochemical conversion of CO_2 focus on the two main oxygenate products obtained from two-electron reactions, which are (the acid-base conjugate) formic acid and formate (HCOOH/HCOO-) and oxalic acid and oxalate (HOOCCOOH/ $-OOC^-COO^-$).[25] For oxalic acid/oxalate the presence/absence of water is important.[26] Other recent developments focus on C2 products and the coupling of renewable electricity with the electrochemical conversion of CO_2.[27–29] The combination of all possible CO_2 reduction reactions (to each possible product) and the hydrogen evolution will form the total cathodic half-reaction (for aqueous electrolytes, in non-aqueous electrolytes the reduction of the appropriate solute will replace it). The CO_2 conversion to formate/formic acid, which usually has the side products of CO and hydrogen gas, is represented by the following equations:

$$CO_2\,(aq) + H_2O\ (l) + 2\,e^- \rightleftarrows HCOO^- + OH^- \quad [1]$$

$$CO_2\,(aq) + H_2O\ (l) + 2\,e^- \rightleftarrows CO + 2OH^- \quad [2]$$

[z]E-mail: Wiebren.deJong@tudelft.nl

$$2H_2O\ (l) + 2\,e^- \rightleftarrows H_2 + 2OH^- \quad [3]$$

As mentioned, one of the main factors that determine product selectivity is the cathode material. Tin (Sn), Indium (In), or lead (Pb) would typically be used as monometallic catalysts for the production of formate in sufficiently alkaline aqueous environments. There are similar materials that are used for the production of carbon monoxide, like silver, with formate and hydrogen as the side products.[30–32] The percentage of each product that is made is defined as the faradaic efficiency:

$$FE_i = \frac{j_i}{j_{total}} \times 100\% \quad [4]$$

Where j_i is the current density for the ith reaction, and j_{total} is the total current density. Note that the FE is purely about selectivity, the interaction with energy efficiency is only in terms of wasted energy producing side products. This can be seen in this definition of energy efficiency (EE):

$$EE_i = \frac{-(\text{Production rate}_i)\cdot \Delta G_i}{(I_{total}\cdot U_{cell})} \times 100\% \quad [5]$$

Where ΔG_i is the Gibbs free energy of reaction to create the product i, I_{total} is the total current, and U_{cell} is the voltage applied to the cell. The rate of production is directly dependent on FE, but the denominator term does not have any direct relation to FE.

One of the main limiting factors in the design of CO_2 electrolyzers is the delivery of enough CO_2 to the surface of the cathode. This problem is often viewed as CO_2 solubility not being high enough at ambient conditions, but it can equally be viewed as the CO_2 having a low mobility in aqueous electrolytes. A popular solution to this problem is the use of gas diffusion electrodes (GDE) where the CO_2 is not kept in solution but is provided in gas phase from behind the electrode,[33–35] which could be seen as tackling the problem from the mobility side as the concentration of CO_2 in the electrolyte does not increase but it is able to reach the electrode faster. Of course, instead of increasing the mobility of CO_2, the concentration can be increased. This has the advantage of requiring only a simple single component electrode rather than an assemble as required with GDEs. Increasing the solubility of CO_2 can be accomplished by at least two methods: using a non-aqueous solvent with high CO_2 solubility[24,36,37] or the application of high pressures.[24,38,39] Compared to GDEs both of these methods are less studied. In the case of non-aqueous solvents there is a challenge to find a solvent that has the desired properties (e.g. low viscosity and high conductivity) at the same time as being cost effective.[24,40] The high pressure method has been noted to be promising given early initial successes, it has produced some of the highest current densities reported in literature,[24,41] despite the relative lack of studies in this area.[24]

Although not many studies focus on high pressure CO_2 reduction, it has a long history. The first work was published in 1914 by Fischer and Przizia.[42] In that initial study, it was found that a ZnHg/Cu electrode was able to produce very high (95%+) FE, even at low pressures, and the formate production rate rose with increasing pressure up to 0.15 A/cm^2 (with 97% FE) at 50 bar (although the potential is not stated). Subsequent work (at much later dates) has followed along in much the same manner. It is understood experimentally that the partial current density of CO_2 reduction, and the achievable FE both generally increase with pressure.[39,41] Temperature effects at elevated pressure are not well studied, but in principle there should be a tradeoff: increasing temperature increases conductivity and reduces cell potential,[43] but decreases CO_2 solubility, and, in fact, there are conflicting results[44,45] - exactly what is expected for a parameter that represents a tradeoff. On electrodes that produce a range of products (primarily Cu based ones) the pressure and potential are both known to effect the product distribution.[38,46,47] These results are always highly dependent on the electrode, and so they are difficult to describe in general terms.

Electrodes that primarily produce formate, CO and H_2 are particularly of interest here. These electrodes are easier to describe as a group (in fact they are grouped as a type of CO_2 reduction catalyst[23]). An increase in pressure increases the maximum achievable FE and partial current density for both formate producing electrodes (Pb, Hg, In, and Sn)[39,44,48,49] and CO producing electrodes (on Ag and Rh).[41,50] In lab scale experiments up to 100% FE at 200 mA/cm^2 for the formate production on Hg, In and Pb at 60 bars,[39] and 80% at 250 mA/cm^2 on Ag for CO production at 30 bar[50] has been demonstrated. The effect of applied potential on CO and formate producing electrodes is similar, but not identical. In the case of formate producing electrodes there is an optimum potential for FE, which falls off at higher or lower potentials.[39,44] CO producing electrodes start at relatively high FE and decrease with increased potential.[41,50] In both cases the partial current density for formate and CO increases with overpotential, until they reach a limiting current at approximately the same potential. Thus, the fall off of FE at high overpotentials is explained by the fact that the HER is not diffusion limited in the same range as the CO_2 reduction is. For these electrodes this is related to the dependence of maximum FE on pressure. As pressure increases the limiting current for CO_2 reduction increases, but the HER is unaffected by pressure, so the max FE increases with pressure.[39] This is somewhat in conflict with Chaplin et al.,[23] where HER is hypothesized to be suppressed by CO_2 electroreduction, but the data available in the literature tend not to support this for CO and formate producing electrodes.[39]

The study of the CO_2 electroreduction into formate and CO at high pressure has produced very impressive results at a lab scale as mentioned above,[39,50] but experiments carried out under more industrial conditions are not quite as impressive (1–2 orders of magnitude lower). In one study with a reactor in a fixed bed configuration with Pb pellets as the cathode only produced a partial current density toward formate of ~1.5 mA/cm^2,[44] indicating that this configuration is likely not appropriate for the CO_2 electroreduction. A more standard parallel plate design achieved 90% FE and 50 mA/cm^2 partial current density at 30 bar on a Sn electrode.[49] It is clear there are still some questions to answer on how exactly to design a high pressure CO_2 electrolyzer – to scale up the results from the lab scale.

Models will be a very important tool in the improvement of the design of such a CO_2 electrolyzer, and are the focus of the present work. Specifically, a macro approach will be used, modeling process conditions. This approach has been applied to electrochemical systems in the past e.g.[51–53] For CO_2 electrolyzers in particular there are models of designs making use of GDEs,[34,35,54–56] solid oxide CO_2 electrolyzers,[57–60] and planar electrode electrolyzers.[61–65] Most of these models fall under the category of diffusion-reaction models, though some are coarser grained plug flow models.[62,63] For diffusion reaction models the details of the bulk electrolyte is one important aspect. The equilibrium between CO_2(aq) – carbonic acid-(bi)carbonate will produce the bulk concentrations given different electrolyte properties and has been included in several models.[56,61,64] More recently the salting out effect of bicarbonate (and other salts) has been considered, this can decrease the solubility of CO_2 by around 20% at atmospheric conditions.[34,66] For planar electrodes the method that CO_2 enters the electrolyte does not matter because the gas can be assumed to be equilibrated with the electrolyte.[61,64] However, for setups with GDEs the way the CO_2 enters the electrolyte is of vital importance. The GDE itself can be treated as flat gas-liquid boundary with the electrode in the same plane,[55,56] as a three dimensional electrode on top of that plane[34,66] or as impermeable surface which directly reacts CO_2 from the gas phase with components of the electrolyte.[35] Beyond how the CO_2 enters the solution, how it reaches the cathode surface, whether through liquid or gas, is also important. This is the diffusion portion of the model, and is governed by Fick's diffusion,[34,54,55,61,64] more rarely by Maxwell-Stefan[56] diffusion (but mainly for gas diffusion, not ionic species), or the dusty gas model[58,60] (for diffusion in porous structures). It can be noted that for a similar electrochemical system (a fuel cell), that Maxwell-Stefan does not produce significant benefits over Fick's law.[67] The electrochemical reactions are the last, but not least, important element that such models must treat. The electrochemical reaction rates have been treated simply as an input to the model,[35,64] but mostly some combination of the Tafel equation or

the Butler-Volmer equation is used to generate them. An interesting choice is whether mass-transport limiting current densities are taken into account by using an explicit limiting value in the model[55,62,63,65] or by trying to predict such limits via the kinetic equations of the model itself.[35,54,56,61] It is preferably for the study of high pressure reactors that the limiting currents be predicted by the model, rather than be an input of the model, since the limiting current is one of the essential elements that a high pressure CO_2 electrolyzer is seeking to alter. A possible further step is to add adsorbed species as another phase in the model, and use Butler-Volmer kinetics in a micro-kinetic model.[56,61] However this method predicts peaking partial current densities, which does not agree the saturating current densities observed in the literature,[39,50] so perhaps a simpler form would be more appropriate until more details of the microkinetics are established.

Here we present a diffusion-reaction model of CO_2 electrolyzers that incorporates the effects of elevated pressure. In all the modelling efforts for CO_2 electrolyzers the only studies to include pressure effects are by Oloman and Li[62,63] and these are quite simple models. More importantly, the pressure in those models has no effect on the electrochemical reactions. Since pressure is one of the few ways of solving the problem of delivering CO_2 to the electrode, the lack of work modeling pressure effects on the electrolyzer is a clear hole in the literature. In the model presented here the pressure is allowed to affect the solubility of CO_2 in the electrolyte, which in turn affects the properties of the electrolyte, and the rates of the electrochemical reactions and their limiting currents (which are predictions of the model rather than inputs). In the following, the model will be explained and validated on data from the literature. The predictions of the model regarding the peak partial current density for CO_2 reduction, FE, energy efficiency, and some economic analysis are presented.

Modeling

A numerical model for the electrochemical conversion of carbon dioxide as function of its (gas phase) pressure has been developed. For a proper numerical description a number of aspects need to be taken into account, that is

(1) the bulk equilibrium reactions involving CO_2, water, and the corresponding ionic species,
(2) the diffusion of the species (CO_2 and the ions) from bulk electrolyte to the cathode surface, and
(3) the electrochemical reaction kinetics of CO_2 to formate (and some side-products) on the surface of the cathode.

The model itself is a system of partial differential equations for (2), for which (1) and (3) give the boundary conditions. A schematic of the model is shown in Figure 1. The system is solved numerically using Matlab, as described in SI4**.**

Bulk solution equilibrium.—To take the contribution of the various species in the electrolyte into account, first the CO_2 solubility as function of the pressure needs to be described. This requires an isotherm model to describe the distribution of CO_2 over the gas phase and the liquid phase. In this work the electrolyte is taken to be potassium bicarbonate, $KHCO_3$, as it is a commonly used electrolyte for CO_2 electroreduction studies (e.g.[39,49]). In the following, a description of the various equilibrium reactions between CO_2, water, bicarbonate, and carbonate is required, which is a function of the CO_2 pressure (or solubility) and the electrolyte concentration.[68,69] In this work the concentration of K^+ and bicarbonate are taken into account according to,[68] modeling the bicarbonate concentration as Cl^- concentration. This is justified by the results of Tang et al. who demonstrated that bicarbonate has nearly the same salting out effect as Cl^- (within 5%), explaining that though bicarbonate is larger than Cl^- the equilibration with HCO_3^- compensates this producing a similar size effect.[70] After the total amount of dissolved CO_2 is determined the equilibrium reactions must be considered. The equilibrium reactions for the

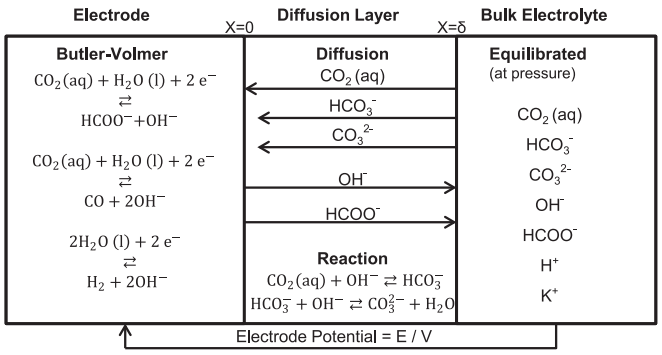

Figure 1. A schematic the model presented in this section. It is made of three parts: the bulk solution portion, the diffusion layer portion, and the electrode surface portion. The bulk solution and electrode surface provide boundary conditions for the diffusion reaction system that comprises the diffusion layer portion. The species depicted in the bulk are equilibrated after an initial concentration is used to determine how much CO_2 can be dissolved (see Bulk solution equilibrium section). The arrows in the diffusion layer represent the species that are allowed to diffuse through the layer in the model and their expected direction of travel (see Diffusion layer section). The surface is governed by three electrochemical reaction which are represented by the Butler-Volmer equation (see Initial and boundary conditions section).

CO_2 - water system are:

$$CO_2\,(aq) + H_2O\ (l) \rightleftarrows H_2CO_3 \quad K_h \qquad [6]$$

$$H_2CO_3\,(aq) \rightleftarrows HCO_3^-\,(aq) + H^+\,(aq) \quad K_0 \qquad [7]$$

$$CO_2^*\ (aq) + H_2O\ (l) \rightleftarrows H^+\,(aq) + HCO_3^-\,(aq) \quad K_1 \qquad [8]$$

$$HCO_3^-\,(aq) \rightleftarrows CO_3^{2-}\,(aq) + H^+\,(aq) \quad K_2 \qquad [9]$$

$$H_2O\ (l) \rightleftarrows OH^-\,(aq) + H^+\,(aq) \quad K_w \qquad [10]$$

with: K_i the equilibrium constant given by the ratio of the equilibrium constants for the forward and backward reaction, $K_{i,F}/K_{i,B}$. CO_2^* (aq) is the concentration of CO_2 and carbonic acid together. The system is assumed be an ideal solution. The values for the equilibrium reaction constants are given in SI1.

Diffusion layer.—For the description of the reactive system two main balances need to be considered, the mass balance and the charge balance, which are:

$$[CO_2] + \left[HCO_3^{2-}\right] + \left[CO_3^{2-}\right] = [C_{carbon}] \qquad [11]$$

$$\left[K^+\right] + \left[H^+\right] - \left[HCO_3^-\right] - 2\left[CO_3^{2-}\right] - \left[OH^-\right] = 0 \qquad [12]$$

The transport of ionic species in an aqueous electrolyte solution is given by the Nernst - Planck equation. In this work the following three contributions are considered:

- Diffusion of the different species (ions and CO_2) across the concentration gradient, ∇C
- Migration of charged ions across the gradient in the electric potential, $\nabla\phi$
- Transport of species as a result of convection in the bulk electrolyte solution, Cv

The overall relation for the flux, $N(k)$ (mole $\cdot\ s^{-1} \cdot m^{-2}$), of a certain species, k, is given by:

$$N\,(k) = -D\nabla C - u\,(k)\,z F C\,(k)\,\nabla\phi + C\,(k)\,v\,(k) \qquad [13]$$

with C: concentration (M), ϕ: electric potential (J), F: Faraday constant (96485 C/mole) u: mobility of the ionic species (m/s), z: the electric

charge of the ionic species (C), and k is an index that refers to different species in the system.

In this work we assume that the bulk electrolyte solution is well mixed and in contact with a stagnant diffusion layer which is in contact with the cathode. This leads to the assumption that the contribution of convective flow of species can be neglected:

$$Cv_x = 0 \quad [14]$$

Next the migration term ($\nabla\phi$) is considered. The most important species in the system (CO_2(aq)) is uncharged, so the electric migration term will have no effect on it. This suggests that it should be neglected, as is common for similar systems.[51,52] The migration term could be important via the (bi)carbonate ions, which indirectly effect the reactions of interest. However, the electrolyte is quite conductive, and the diffusion layer will be more conductive than the bulk, due the OH^- formed at the electrode. Thus, the migration term will be negligible, especially for low currents, but even at high currents it would be a correction to an indirect effect. Therefore, in this work the migration term is neglected. After eliminating migration and advection, the governing contributions for the transport of species are as a result of a difference in the concentration alone, which is treated by Fick's diffusion equation (neglecting cross terms). If the following reactions:

$$CO_2\,(aq) + OH^- \rightleftarrows HCO_3^- \quad K_3 \quad [15]$$

$$HCO_3^- + OH^- \rightleftarrows CO_3^{2-} + H_2O \quad K_4 \quad [16]$$

that are in equilibrium in the bulk continue in the diffusion layer (being base balanced version of Eqs. 6 and 9) they will provide source terms for each species. Altogether, the following equations are solved numerically with the appropriate initial and boundary conditions:

$$\partial/\partial t\left[CO_2\,(aq)\right] = D_{CO_2}\,\partial^2/\partial x^2\left[CO_2\,(aq)\right] - k_{3,F}\left[CO_2\right]\left[OH^-\right] + k_{3,B}\left[HCO_3^-\right] \quad [17]$$

$$\partial/\partial t\left[HCO_3^-\right] = D_{HCO_3^-}\,\partial^2/\partial x^2\left[HCO_3^-\right] + k_{3,F}\left[CO_2\right]\left[OH^-\right] - k_{3,b}\left[HCO_3^-\right] + k_{4,F}\left[HCO_3^-\right]\left[OH^-\right] - k_{4,B}\left[CO_3^{2-}\right] \quad [18]$$

$$\partial/\partial t\left[CO_3^{2-}\right] = D_{CO_3^{2-}}\,\partial^2/\partial x^2\left[CO_3^{2-}\right] + k_{4,F}\left[HCO_3^-\right]\left[OH^-\right] - k_{4,B}\left[CO_3^{2-}\right] \quad [19]$$

$$\partial/\partial t\left[OH^-\right] = D_{OH^-}\,\partial^2/\partial x^2\left[OH^-\right] + k_{3,F}\left[CO_2\right]\left[OH^-\right] + k_{3,B}\left[HCO_3^-\right] - k_{4,F}\left[HCO_3^-\right]\left[OH^-\right] + k_{4,B}\left[CO_3^{2-}\right] \quad [20]$$

with: D: Fick's diffusion coefficient (m^2/s).

The values for the diffusion coefficients of the various components in water are listed in SI1.

Initial and boundary conditions.—*Initial conditions (IC).*—At t<0, that is before the simulation (or the experiment) is started only the electrolyte solution is present. In other words, the diffusion layer is no different than the bulk initially. The concentration of the various species in the electrolyte solution is given by the equilibrium relations, Eqs. 6 to 10.

Boundary condition 1 (BC 1).— The first boundary condition is that at the edge of the diffusion layer the concentrations of all species is equal to their bulk concentration as calculated, under a given CO_2 pressure. This gives a Dirichlet boundary condition between the diffusion layer and the bulk (see SI4).

Boundary condition 2 (BC 2).— The second boundary condition is specified by the relation between the current (density) and the applied potential on the cathode. This is because the flux of reactants and products from electrochemical reactions can be directly related to the partial current density associated with the appropriate reaction. The relationship between current and voltage in an electrochemical reaction is given by the Butler-Volmer equation (with the reverse reaction omitted):

$$j_i = j_{0,i}\exp\left[\frac{-\alpha_{c,i}n_iF}{RT}\eta_i\right] \quad [21]$$

with j: the current density (A/m^2), j_0: the exchange current density (A/m^2), α: the charge transfer coefficient, n: the number of electrons involved in the reaction, and η: the overpotential (V), or:

$$\eta_i = U - U_{eq,i} \quad [22]$$

With U: the applied potential, and U_{eq} the equilibrium potential for a given reaction according to standard potentials at pH 7[71] (see SI1 for equilibrium potentials). The exchange current density is defined as:

$$j_{0,i} = C_m n_i k_i F \quad [23]$$

With C_m being the concentration of the reactant m at the cathode in reaction i (either CO_2 or H_2O) and k_i being the reaction constant. The current can then be related to the flux of chemical species according to:

$$\frac{\partial}{\partial t}[m] = \pm\frac{\nu_m j_i}{Fn_i} \quad [24]$$

ν_m is the stoichiometric coefficient from product or reactant m for reaction i, and the sign being dependent on whether m is a product or a reactant. Thus, each reaction has its own partial current density. Each Butler-Volmer equation requires two parameters, the charge transfer parameter and the reaction constant. These parameters are determined by fitting experimental data in the Tafel region. This approach is accurate for at least some electrochemical systems,[52,72] and is simpler than trying to model surface coverages. It is interesting to note that although this assumes that the 3 reactions are independent on the surface, they still interact via the concentration of species near the surface of electrode. For example, the produced OH^- can limit the amount of CO_2 reaching the electrode surface. Altogether, the three Butler-Volmer equations give a Neuman boundary condition (see SI4) for the diffusion-reaction system at the electrode surface.

Allowing the concentration dependence of the electrochemical kinetics is another point to highlight. In the first place it provides a transition between the region where the reaction is controlled by the electrokinetics to the region where it is mass transfer limited. When the partial current density peaks this value is taken to be the limiting partial current density. It provides a basis to predict the limiting current from the model, rather than using it as a hard coded input.

Energy input.—The theoretical cell potential required to perform the CO_2 to formic acid electroreduction on the cathode and the oxygen evolution on the anode is 1.43 V.[73] Thus, the minimum amount energy per kg of formate (molar mass = 45 g/mol):

$$E_{\min} = -nFU_{eq} = 276\ (kJ/mol) = 1703\,(Wh/kg\ formate) \quad [25]$$

The energy efficiencies of the reaction reported in the literature are on the order of 50%,[73,74] so the overall efficiency can be estimated to be (taking into account FE):

$$E_{\text{eff.min}} = 1703\ (\text{Wh/kg formate}) / (50\%) = 3406\ (\text{Wh/kg formate}) = 3.4\ (\text{kWh/kg formate}) \quad [26]$$

Results and Discussion

The aspects of the solubility, diffusion, and the electrochemical reaction of CO_2 in a system composed of an aqueous electrolyte in contact with a metal cathode have been described numerically.

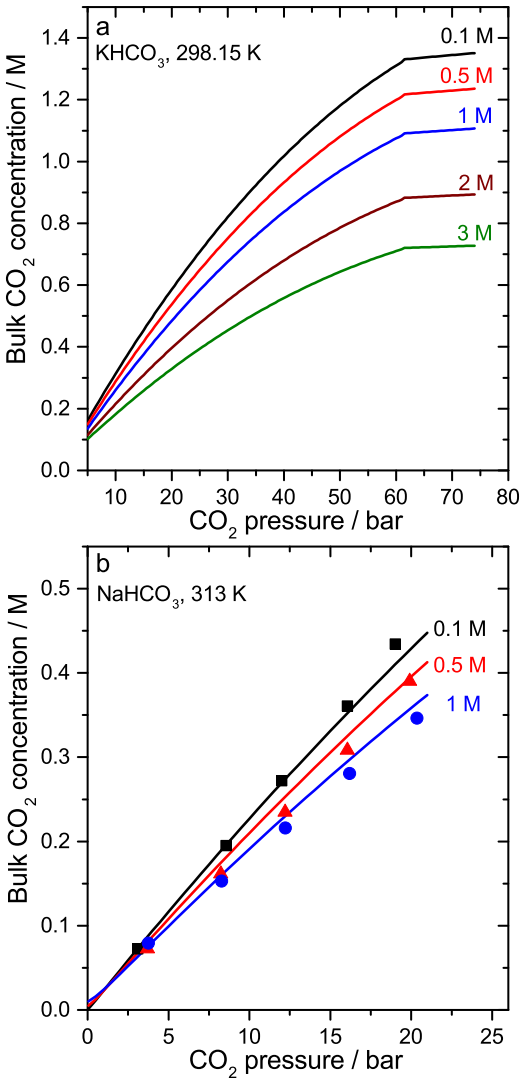

Figure 2. Solubility, concentration of CO_2 in potassium bicarbonate electrolyte as a function of the pressure, up to 73 bar for several concentrations of potassium bicarbonate at 298.15 K (a) and sodium bicarbonate at 313K (b). The model is the curves, and the data points in (b) from Xiaoying et al.[78] The curves are produced by following Duan et al.[68] and modeling the bicarbonate concentration as Cl- since they have similar salting out effects.[70]

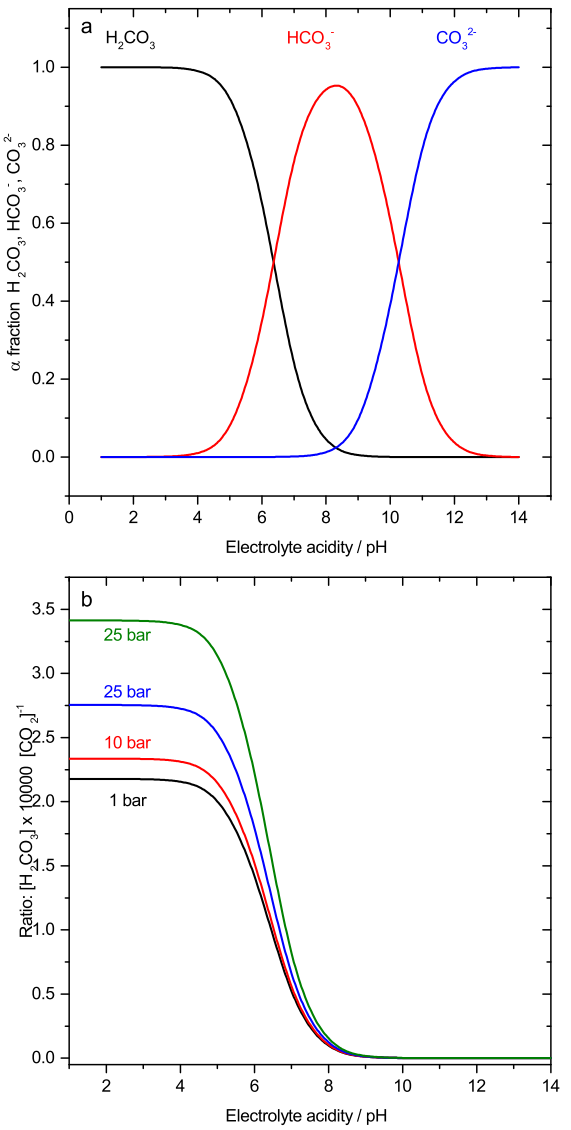

Figure 3. Ratio of H_2CO_3 to CO_2 solubilized in water as function of the pH for four different gas phase CO_2 pressures.

The main purpose is to study the effect of the CO_2 pressure on the electrochemical conversion of CO_2 to formate/formic acid. There are only a few papers reporting detailed experimental data for the effect of the CO_2 pressure on the electrochemical conversion of CO_2 in aqueous electrolyte solutions.[23,24,39,41,50] A few papers evaluate the effect of the operating conditions for the formation of formate[23,50] or carbon monoxide.[24,41]

The most obvious predictions of this model are as a result of its treatment of the bulk electrolyte. Specifically the pressure effects on the solubility of CO_2 are seen, and the effects increased CO_2 solubility has on the pH and concentration of ionic species in the electrolyte as a result. This is not surprising as the whole idea of running a CO_2 electrolyzer at high pressures is to alter the CO_2 solubility of the bulk electrolyte. Figure 2 shows the CO_2 solubility of a bicarbonate electrolyte calculated as described in Bulk solution equilibrium section for several different potassium bicarbonate concentrations at 298.15 K (and 313 K to compare the literature data). As expected, it rises with pressure and saturates when CO_2 becomes a liquid, that is above 60 bar (at room temperature) or supercritical (at 31.10°C and 73.8 bars). Additionally, the salting out effect of sodium bicarbonate is readily apparent, a 3 M solution of sodium bicarbonate having nearly half as much dissolved CO_2 as a 0.1 M solution. This is accompanied by a resistivity change from ~5 Ωcm for 3 M to ~100 Ωcm for 0.1 M.[75] The solubility of CO_2 is not the only important quantity of the bulk electrolyte that can be predicted, another important point is seen in Figure 3, which shows the carbonic acid-bicarbonate-carbonate equilibrium. As explained in bulk solution equilibrium section, the concentration of the three ions are in equilibrium with each other and the CO_2(aq). Some amount of the CO_2 gets converted into the other species. However, especially note Figure 3b, which shows a ratio of the amount of dissolved CO_2 and carbonic acid vs. pH. The amount of dissolved CO_2 is always much higher than the amount of carbonic acid. Thus, at all pHs there is plenty of CO_2 (aq) available. Since increasing CO_2(aq) concentration is the main purpose of operating a CO_2 electrolyzer at high pressure, this is an important point. It is also interesting to note that it indicates the active species in the CO_2 reduction is CO_2 and not bicarbonate.

Also of interest, the bulk pH of the electrolyte decreases with CO_2 pressure, as can be seen in Figure 4a. However, even at quite low concentrations of $KHCO_3$ (e.g. 0.1 M) the pH does not go below 5.4 (at 25°C). The significance of this is that it will determine the product distribution between formate and formic acid. In Figure 5

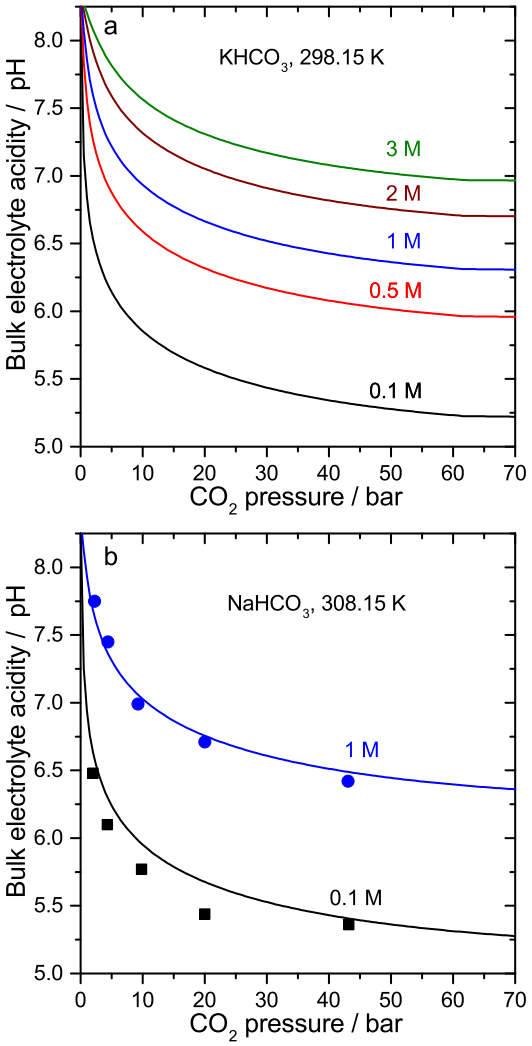

Figure 4. pH of the bulk electrolyte as a function of the applied pressure of CO_2 for several different concentrations of potassium bicarbonate at 298.15 K (a) and sodium bicarbonate at 308.15 K (b). The curves are generated by the model, and the data points in (b) are from Li et al.[76] for the pH of 0.1 and 1 mol/kg sodium bicarbonate at 317 K. Low concentration solutions of bicarbonate do become acidic at elevated pressure, but only slightly. For further explanation of this figure see SI3.

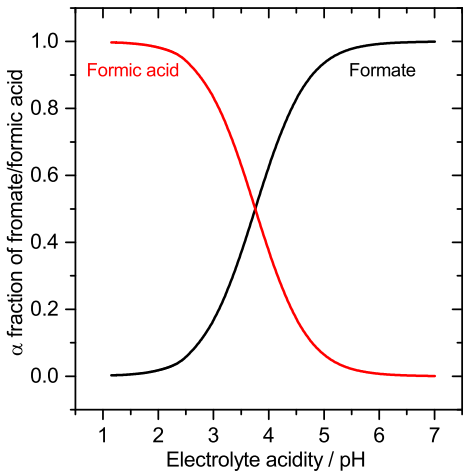

Figure 5. Distribution of formate/formic acid in an aqueous solution as a function of pH. Note the relatively low pH that must be maintained before a majority of product would be formic acid.

the fraction of formate/formic acid is shown vs. pH (see SI2 for calculations), and it can be seen that all bulk pH values attainable in a bicarbonate electrolyte in a high pressure CO_2 electrolyzer will tend to favor formate over formic acid (even those that are slightly acidic). If formic acid is desired then a pH of less than 2 to 3 should be targeted for the electrolyte. Additionally, notice the data points in Figure 4b, these points are of the pH of sodium bicarbonate solution at 308 K,[76] which in terms of CO_2 solubility and pH at least, should be very similar to the potassium version. With that understood, the agreement with this experimental data further validates the model's bulk electrolyte components independent of the further electrochemical results.

On the electrochemical side, the numerical model uses the relation between the partial current density and the applied potential as the main input. This is done through boundary conditions (BC 2), which relates the voltage to the consumption and production of the individual components on the metal cathode surface according to the Butler-Volmer equation. In Figure 6 the partial current density as a function of the applied potential is shown for two CO_2 pressures (5 and 40 bar) using an indium cathode. With respect to the effect of the CO_2 pressure it can be seen that for hydrogen the partial current density as function of the potential is independent of the applied CO_2 pressure. On the other hand, for both formate and carbon monoxide there is clear effect of the pressure. For formate and carbon monoxide, there is a small effect on the initial slope at a low potential and a low current density. The most significant effect of the pressure is on the value for the limiting current density. The value for the limiting current density increases with an increase in CO_2 pressure for both formate and carbon monoxide, as expected.

An interesting note here is that in the model the limiting CO_2 reduction partial current density is dependent on the surface concentration of CO_2(aq) (it will limit when the concentration approaches 0). In terms of the model's parameters this is determined by the diffusion layer thickness, which was fit to just the lowest pressure data (5 bar) from Todoroki et al.[39] by selecting a diffusion layer thickness which caused the modeled limiting current to match the experimental value. The ratio between the limiting CO and formate currents is determined by the electrochemical kinetics which are fit by least squares to the same 5 bar data, but using only the values below the limiting current (in the range of -1 to -1.4 V vs Ag/AgCl). With just these parameters fit, on only the 5 bar data, the limiting formate and CO partial current density matches the values from the literature very well, as can be seen in Figure 7. The only exception is the point at 20 bar, which can be determined to be an outlier with the insight of this model.

One of the main parameters is the FE for the different products that can be formed during the electrochemical reaction. The dependence of the partial current density on the potential for the three components has a strong influence on the FE. In Figure 8 the FE is given as a function of the (total) current density for a CO_2 pressure of 5 and 40 bar again. A comparison is made between the FE calculated with the model and data from the literature.[39] It can be seen that there is a clear relation between the FE for the main product, formate, and the hydrogen formed during the reaction. Above a current density of around 80 mA/cm^2 at 5 bar and 400 mA/cm^2 at 40 bar the FE for formate starts to decrease while the FE for hydrogen starts to increase. This is due to the limiting current density being reached for formate, and the HER still being non-mass transport limited (as can be seen by comparing to Figure 6).

In terms of partial current density, the agreement of the model with data at 5 bar is clearly much better than for data at 40 bar. This larger error is mostly due to the currents which are high, but not limiting (in the range of -1.2 to -1.3 V). For only the data points which are not limiting current the R-square is 0.92 for 5 bar data (which was used to generate the fit) to -0.3 for 40 bar data (Figure 6). This is clearly not desirable, but the model can be said to predict the patterns of the data, and this can be seen in the FE plots (Figure 8). The agreement of the model with the data is significantly better in terms of FE, at 5 bar the R-square is 0.99 and at 40 bar it is 0.98. The question as to why the partial current density prediction for 40 bar

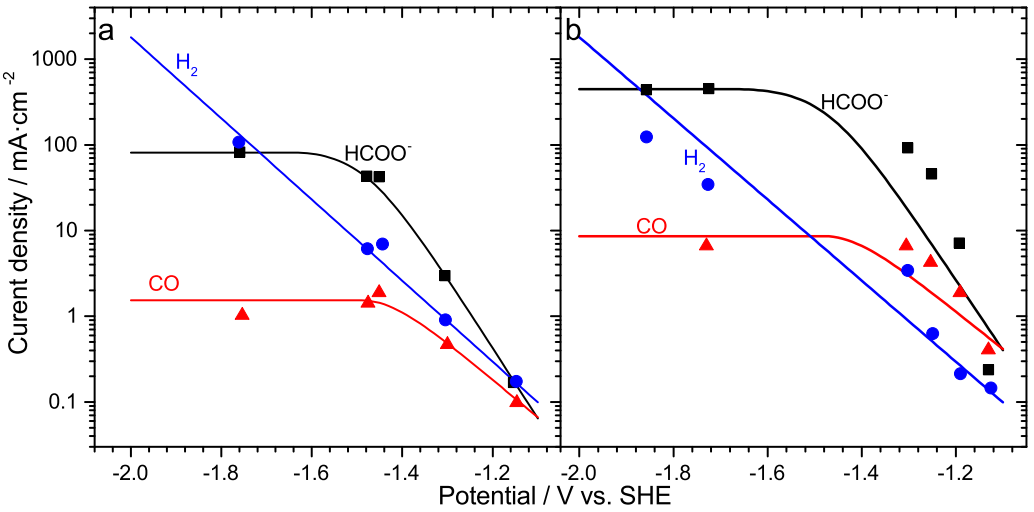

Figure 6. Tafel plot with the partial current density as function of the applied potential for the electrochemical conversion of CO_2 to formate on an Indium (In) cathode at 298.15 K, 5 bar (a) and 40 bar (b). Markers are experimental values from the literature[39] and lines are the values predicted by the model. The different curves for hydrogen (blue), formate (black) and carbon monoxide (red) are noted on the figure.

is poor remains unanswered. It is most likely due to a phenomenon unaccounted for in the model. This phenomenon must primarily effect the electrokinetics and effect the limiting current uniformly (if at all), since the limiting currents fit well. Additionally it must effect both CO_2 electroreduction reactions equally, since the FE fits well. To understand the possibilities of why the model does not predict these values well consider how pressure could affect the electrokinetics: CO_2 concentration, pH change (from increased CO_2 concentration), and temperature increase (from ohmic heating at higher current densities, achievable due to higher CO_2 concentration). The direct effect of a higher concentration of CO_2 is taken into account of in the model already via the Butler-Volmer equation. However, unlike CO_2 concentration, temperature and pH are not taken into account, and doing so would be challenging since they both have effects on the kinetics of the reaction beyond the obvious shifting of equilibrium potential.[43] A local temperature increase might be the cause of the difference; its effect would depend on several factors including the shape of the cell. The pH is ~0.5 lower at 50 bar than it is at 5 bar, so the equilibrium potential would ~30 mV lower, but this does not account for the higher Tafel slope at 40 bar. The pH is also known to affect the kinetics of the CO_2 electroreduction, but it effects selectivity as well,[24,33] and since the FE fits this seems unlikely. One possible explanation is that the mechanism of a reaction step common to both CO_2 electroreduction reactions changes at high pressure/CO_2 concentration (e.g. the adsorption of CO_2). Unfortunately, there is not enough information, in the literature (or in this model) to determine the cause with certainty. This point requires further (experimental) study at elevated pressure in three electrode cells to resolve. A final point on the model's predictive power is that it is not extremely sensitive to any of the physical variables taken from the literature, this can be seen in SI5. Overall, considering that the limiting current density and FE are predicted very well, the performance of the model in comparison to the literature is good.

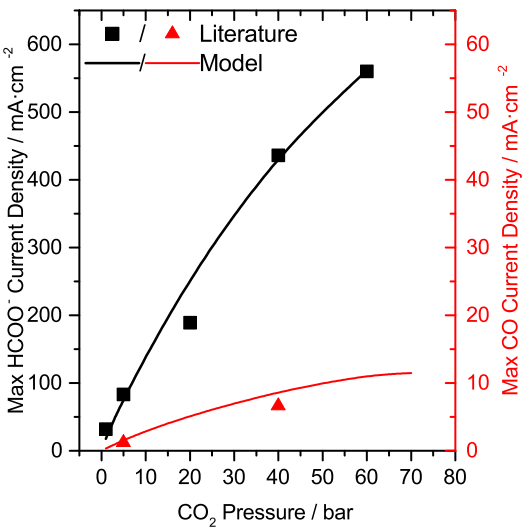

Figure 7. A comparison of the limiting partial current density for formate and CO production vs. applied CO_2 pressure between experimental literature values for In[39] and those predicted by the model at 298.15 K. Essentially, the relation shows that limited partial current density continues to increase with CO_2 pressure.

The model is able to predict the trends at 40 bar well enough that it is interesting to look at some further predictions made by the model, at least qualitatively. It has already been seen that the limiting partial current density (alternately, this could be called the maximum production rate) for formic acid increases with pressure. Similarly, Figure 9 shows the maximum attainable FE as a function of pressure, which can be seen to be relatively insensitive to pressure above 10 bar. This is important because it means for academic experimentation lower pressures of around 10 bars might suffice to see effects on FE. However, there are practical reasons to increase an industrial CO_2 electrolyzer's pressure, such as a high current density (see Figure 6) to make the reactor economically feasible.

The economics of a CO_2 electrolyzer can also be examined with this model. For example in Energy input section an estimate of the electric power cost per kg is made of 3.3 kWh. To look at this the model is used to make some estimates of the energy costs involved to produce formic acid electrochemically, which can be seen in Figure 10 (plotted for several different pressures). The anode is assumed to be 100% oxygen evolution and not mass transfer limited with Tafel parameters as found in the literature.[77] For the Omhic losses, an inter-electrode gap of 10 mm and resistivity of $\rho = 22.3$ Ωcm (for a potassium bicarbonate concentration of 0.5 M[75]).

As can be seen the minimum energy cost possible is 3.7 kWh/kg, which is achieved and not significantly improved upon above 10 bar. This is a reasonable number as it is similar to the estimated value above (3.3 kWh/kg). The gross profit is a quite different statistic than

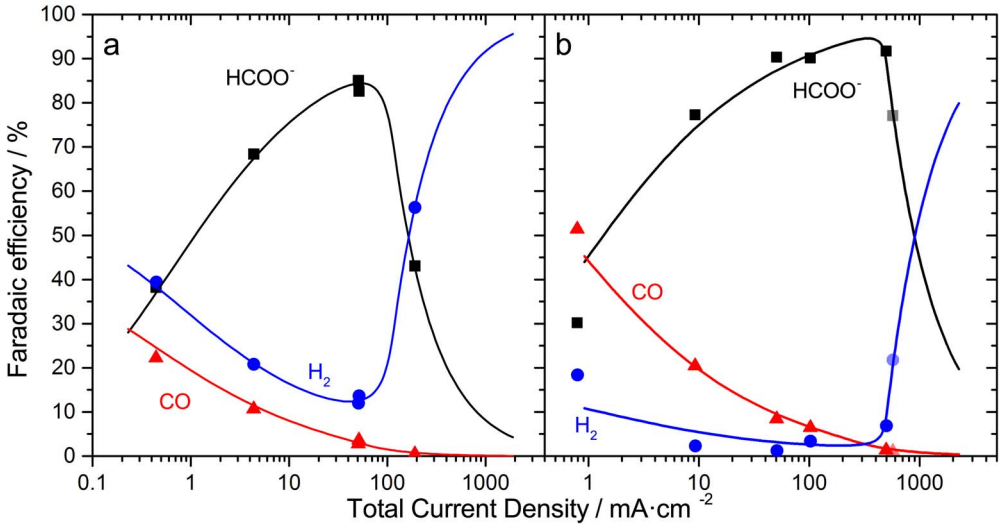

Figure 8. Current efficient as a function of the current density for the production of formate, with as two main by-products carbon monoxide and hydrogen. Results are for an Indium (In) cathode, at 298.15 K and at a pressure of 5 bar (a) and 40 bar (b). Lines are calculated with the numerical model and markers are experimental data from the literature.[39] The different curves for hydrogen (blue), formate (black) and carbon monoxide (red) are noted on the figure. Note: the semi-transparent data points in (b) are from a set which is missing a value for CO partial current density, this point is what the FEs would be if the CO partial current density is simply projected from the previous values.

the cost, as it incorporates the cost of CO_2, price of formic acid, and the specific rate of production. Figure 11 shows the expected gross profit per year for a 10 m^2 reactor. Clearly, the situation is not great for this particular electrode material. However, it can still be instructive as it illustrates the difference between maximum production and maximum efficiency. Essentially, for cheaper electricity it is preferable to operate the reactor closer to the maximum production rate, and as the electricity price increases the optimum point moves toward the maximum efficiency point; in general it is preferable to operate it somewhere in-between. This pattern will be true for any combination of electricity cost, CO_2 cost and formic acid price that produce a profit. Also note the inset in Figure 11, which shows the maximum gross yearly profit as a function of pressure (for an electricity cost of 1 c/kWh). It can be seen that profit follows the same pattern as CO_2 solubility and maximum partial current density (see Figure 2 and Figure 7), which shows the importance of maximum partial current density as an important performance indicator.

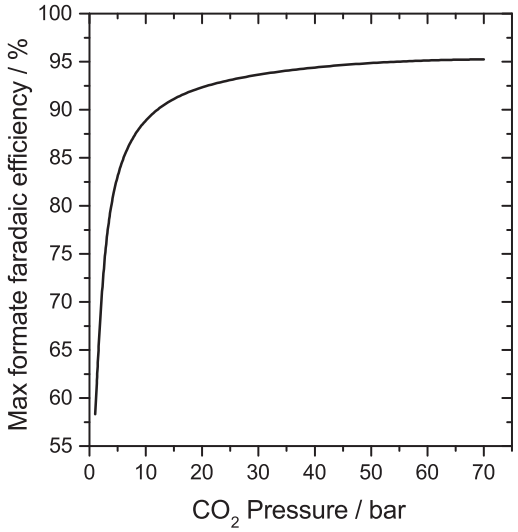

Figure 9. The maximum FE vs. applied CO_2 pressure predicted by the model for the data fit to the In electrode[39] at 298.15 K.

Conclusions

In this work a model was developed that uses a diffusion-reaction system to describe a high pressure CO_2 electrolyzer. The model was validated by and used to explore data from the literature. This model includes elements to model the electrode surface, the diffusion layer, and the bulk solution. The bulk electrolyte portion of the model was validated by comparing the model pH and CO_2 solubility with experimental values from the literature. This portion of the model showed a few interesting results. First, any electrolyzer running in a bicarbonate solution is definitely producing formate as a product. Also, that the there is always significantly more aqueous CO_2 than bicarbonate making it unlikely that bicarbonate is the active species in the

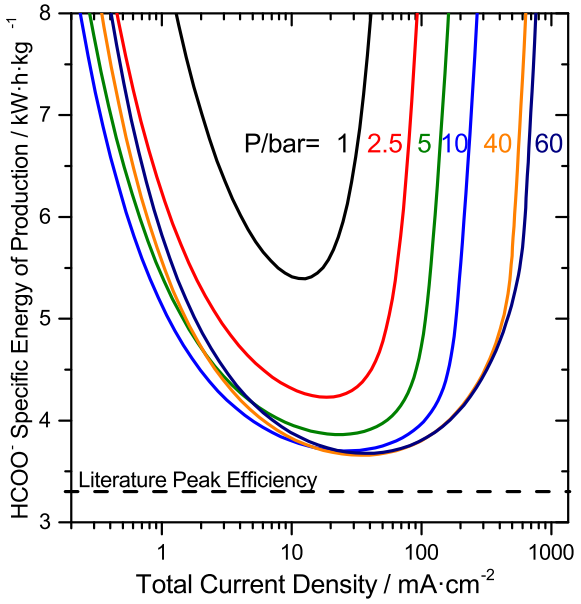

Figure 10. The energy efficiency of the reaction over a range of total current densities, for several different pressures (labeled on the figure, in different colors), as predicted by the model for the In electrode.[39] Very little gain in the minimum energy density is achieved above 10 bar.

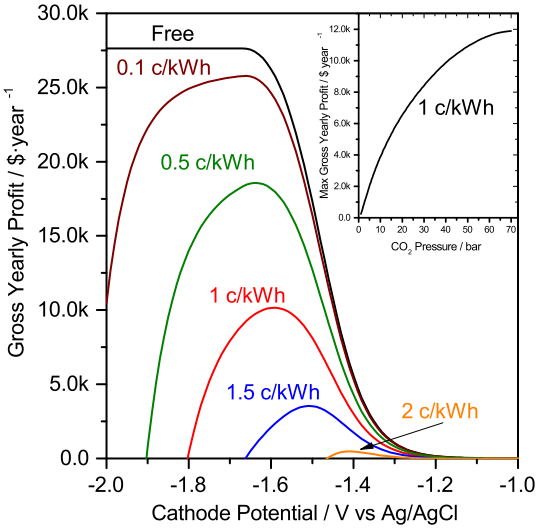

Figure 11. Predicted gross profit per year as a function of the total current density for a 10 m^2 reactor for several different prices of electricity (as noted on the figure). As representative numbers, the pressure is 40 bar, the resistivity of the electrolyte is 25 Ωcm,[75] the inter-electrode gap is 0.1 cm, an anode the same area as the cathode with an oxygen evolution reaction exchange current density of 0.404 mA/cm^2 and Tafel slope of 0.13 V/decade,[77] the cost of CO_2 is $25/ton and the price of formic acid is $850/ton (which are highly optimistic prices).

reaction. Further, the overall model is shown to be in agreement with literature data. In particular the model predicts the limiting current densities of both carbon monoxide and formate well, by only setting a single parameter - the diffusion layer thickness, which is fit to just one data point. In the non-limiting region the model at 5 bar produces very close agreement. However for non-limiting currents at 40 bar the match is worse in terms of partial current density. Given this, it is interesting that the model predicts the FE very well at both pressures. The goodness of fit is essentially unchanged between 5 and 40 bar data for FE (going from 0.99 R-square to 0.98), even though the fit was only done on the 5 bar data. The model shows that current density should be the primary parameter that is affected strongly by pressure. Both FE and energy efficiency are relatively insensitive to pressure above 10–20 bar, but the maximum partial current density does keep increasing with pressure. This is interesting from a practical point of view, since it means that relatively moderate high pressure experimental set-ups could be enough to see important effects. However, for industrial purposes higher pressures are always interesting, since higher specific production is more profitable. The model was used to show a trade-off between efficiency and production rate, and that there will be an economic optimum somewhere between the two in all but the extreme cases. In sum, this work shows the power of a 1-dimensional model to explain the operation of a high pressure CO_2 electrolyzer. In future work modest improvements could be made to this model to see the effects of parameters like temperature, not with a goal to improve accuracy per se, but to expand the insights provided and guide electrolyzer design.

Acknowledgments

The project this work was carried out as part of (TEEI116076: Direct electrochemical conversion of CO_2 to formic acid (P2FA)) is being carried out with subsidy from the Dutch Ministry of Economic Afairs, under the scheme Joint Industry Projects, executed by RVO (Rijksdienst voor Ondernemend Neder-land). TJHV acknowledges NWO-CW (Chemical Sciences) for a VICI grant.

ORCID

Andrew R. T. Morrison https://orcid.org/0000-0001-6015-1677
Wiebren de Jong https://orcid.org/0000-0002-9943-9667

References

1. M. Allen, M. Babiker, Y. Chen, H. de Coninck, S. Connors, R. van Diemen, O. P. Dube, K. Ebi, F. Engelbrecht, M. Ferrat, J. Ford, P. Forster, S. Fuss, T. Guillen, J. Harold, O. Hoegh-Guldberg, J.-C. Hourcade, D. Huppmann, D. Jacob, K. Jiang, T. G. Johansen, M. Kainuma, K. de Kleijne, E. Kriegler, D. Ley, D. Liverman, N. Mahowald, V. Masson-Delmotte, R. Matthews, R. Melcher, R. Millar, K. Mintenbeck, A. Morelli, W. Moufouma-Okia, L. Mundaca, M. Nicolai, C. Okereke, M. Pathak, A. Payne, R. Pidcock, A. Pirani, E. Poloczanska, H.-O. Pörtner, A. Revi, K. Riahi, D. C. Roberts, J. Rogelj, J. Roy, S. Seneviratne, P. R. Shukla, J. Skea, R. Slade, D. Shindell, C. Singh, W. Solecki, L. Steg, M. Taylor, P. Tschakert, H. Waisman, R. Warren, P. Zhai, and K. Zickfeld, Global Warming of 1.5°C an IPCC special report on the impacts of global warming of 1.5°C above pre-industrial levels and related global greenhouse gas emission pathways, in the context of strengthening the global response to the threat of climate change, sustainable development, and efforts to eradicate poverty - Summary for Policymakers, in *IPCC report*, Incheon, Korea (2018).
2. G. A. Olah, T. Mathew, A. Goeppert, and G. K. Surya Prakash, *Topics in Catalysis*, **61**, 522 (2018).
3. A. Tremel, P. Wasserscheid, M. Baldauf, and T. Hammer, *International Journal of Hydrogen Energy*, **40**, 11457 (2015).
4. A. Álvarez, A. Bansode, A. Urakawa, A. V. Bavykina, T. A. Wezendonk, M. Makkee, J. Gascon, and F. Kapteijn, *Chemical Reviews*, **117**, 9804 (2017).
5. G. Centi, E. A. Quadrelli, and S. Perathoner, *Energy & Environmental Science*, **6**, 1711 (2013).
6. A. Sternberg, C. M. Jens, and A. Bardow, *Green Chemistry*, **19**, 2244 (2017).
7. D. Milani, R. Khalilpour, G. Zahedi, and A. Abbas, *Journal of CO_2 Utilization*, **10**, 12 (2015).
8. A. Dutta, S. Farooq, I. A. Karimi, and S. A. Khan, *Journal of CO_2 Utilization*, **19**, 49 (2017).
9. D. H. König, M. Freiberg, R.-U. Dietrich, and A. Wörner, *Fuel*, **159**, 289 (2015).
10. H. Kondziella and T. Bruckner, *Renewable and Sustainable Energy Reviews*, **53**, 10 (2016).
11. T. Hirata, H. Nagayasu, T. Yonekawa, M. Inui, T. Kamijo, Y. Kubota, T. Tsujiuchi, D. Shimada, T. Wall, and J. Thomas, *Energy Procedia*, **63**, 6120 (2014).
12. O. Miyamoto, C. Maas, T. Tsujiuchi, M. Inui, T. Hirata, H. Tanaka, T. Yonekawa, and T. Kamijo, *Energy Procedia*, **114**, 5616 (2017).
13. M. Götz, J. Lefebvre, F. Mörs, A. McDaniel Koch, F. Graf, S. Bajohr, R. Reimert, and T. Kolb, *Renewable Energy*, **85**, 1371 (2016).
14. M. Bailera, P. Lisbona, L. M. Romeo, and S. Espatolero, *Renewable and Sustainable Energy Reviews*, **69**, 292 (2017).
15. S. Perathoner and G. Centi, *Journal of the Chinese Chemical Society*, **61**, 719 (2014).
16. M. Iglesias Gonzalez, B. Kraushaar-Czarnetzki, and G. Schaub, *Biomass Conversion and Biorefinery*, **1**, 229 (2011).
17. A. Galadima and O. Muraza, *Journal of Natural Gas Science and Engineering*, **25**, 303 (2015).
18. S. Jasper and M. El-Halwagi, *Processes*, **3**, 684 (2015).
19. P. Tian, Y. Wei, M. Ye, and Z. Liu, *ACS Catalysis*, **5**, 1922 (2015).
20. O. Yishai, S. N. Lindner, J. Gonzalez de la Cruz, H. Tenenboim, and A. Bar-Even, *Current Opinion in Chemical Biology*, **35**, 1 (2016).
21. A. K. Singh, S. Singh, and A. Kumar, *Catalysis Science & Technology*, **6**, 12 (2016).
22. C. M. Jens, K. Nowakowski, J. Scheffczyk, K. Leonhard, and A. Bardow, *Green Chemistry*, **18**, 5621 (2016).
23. R. P. S. Chaplin and A. A. Wragg, *Journal of Applied Electrochemistry*, **33**, 1107 (2003).
24. J.-P. Jones, G. K. S. Prakash, and G. A. Olah, *Israel Journal of Chemistry*, **54**, 1451 (2014).
25. G. Feng, W. Chen, B. Wang, Y. Song, G. Li, J. Fang, W. Wei, and Y. Sun, *Chemistry, an Asian journal*, (2018).
26. M. C. Figueiredo, I. Ledezma-Yanez, and M. T. M. Koper, *ACS Catalysis*, **6**, 2382 (2016).
27. D. R. Kauffman, J. Thakkar, R. Siva, C. Matranga, P. R. Ohodnicki, C. Zeng, and R. Jin, *ACS Applied Materials & Interfaces*, **7**, 15626 (2015).
28. W. Zhang, Y. Hu, L. Ma, G. Zhu, Y. Wang, X. Xue, R. Chen, S. Yang, and Z. Jin, *Advanced Science*, **5**, 1700275 (2017).
29. Y. Mi, X. Peng, X. Liu, and J. Luo, *ACS Applied Energy Materials*, (2018).
30. Y. Hori, in *Modern Aspects of Electrochemistry*, C. G. Vayenas, R. E. White, and M. E. Gamboa-Aldeco, Editors, p. 89, Springer New York, New York, NY (2008).
31. Y. Hori, in *Handbook of Fuel Cells*, A. L. Wolf Vielstich and Hubert A. Gasteiger, Editor (2010).
32. Y. Hori, H. Wakebe, T. Tsukamoto, and O. Koga, *Electrochimica Acta*, **39**, 1833 (1994).
33. M. N. Mahmood, D. Masheder, and C. J. Harty, *Journal of Applied Electrochemistry*, **17**, 1159 (1987).
34. C.-T. Dinh, T. Burdyny, M. G. Kibria, A. Seifitokaldani, C. M. Gabardo, F. P. García de Arquer, A. Kiani, J. P. Edwards, P. De Luna, O. S. Bushuyev, C. Zou, R. Quintero-Bermudez, Y. Pang, D. Sinton, and E. H. Sargent, *Science*, **360**, 783 (2018).

35. K. Wu, E. Birgersson, B. Kim, P. J. A. Kenis, and I. A. Karimi, *Journal of The Electrochemical Society*, **162**, F23 (2015).
36. O. Aschenbrenner and P. Styring, *Energy & Environmental Science*, **3**, 1106 (2010).
37. T. Saeki, K. Hashimoto, N. Kimura, K. Omata, and A. Fujishima, *Journal of Electroanalytical Chemistry*, **404**, 299 (1996).
38. K. Hara, A. Tsuneto, A. Kudo, and T. Sakata, *Journal of The Electrochemical Society*, **141**, 2097 (1994).
39. M. Todoroki, K. Hara, A. Kudo, and T. Sakata, *Journal of Electroanalytical Chemistry*, **394**, 199 (1995).
40. N. V. Rees and R. G. Compton, *Energy & Environmental Science*, **4**, 403 (2011).
41. K. Hara and T. Sakata, *Bulletin of the Chemical Society of Japan*, **70**, 571 (1997).
42. F. Fischer and O. Prziza, *Berichte der deutschen chemischen Gesellschaft*, **47**, 256 (1914).
43. A. J. Bard, L. R. Faulkner, J. Leddy, and C. G. Zoski, *Electrochemical methods: fundamentals and applications*, wiley New York (1980).
44. F. Köleli and D. Balun, *Applied Catalysis A: General*, **274**, 237 (2004).
45. E. J. Dufek, T. E. Lister, S. G. Stone, and M. E. McIlwain, *Journal of The Electrochemical Society*, **159**, F514 (2012).
46. R. Aydın, H. Ö. Doğan, and F. Köleli, *Applied Catalysis B: Environmental*, **140–141**, 478 (2013).
47. R. Kas, R. Kortlever, H. Yılmaz, M. T. M. Koper, and G. Mul, *ChemElectroChem*, **2**, 354 (2015).
48. O. Scialdone, A. Galia, G. L. Nero, F. Proietto, S. Sabatino, and B. Schiavo, *Electrochimica Acta*, **199**, 332 (2016).
49. F. Proietto, B. Schiavo, A. Galia, and O. Scialdone, *Electrochimica Acta*, **277**, 30 (2018).
50. K. Hara, A. Kudo, and T. Sakata, *Journal of Electroanalytical Chemistry*, **391**, 141 (1995).
51. K. Scott, in *Modern Aspects of Electrochemistry*, R. E. White, J. O. M. Bockris, and B. E. Conway, Editors, p. 1, Springer US, Boston, MA (1995).
52. E. J. Podlaha, C. Bonhôte, and D. Landolt, *Electrochimica Acta*, **39**, 2649 (1994).
53. A. T. Marshall and A. Herritsch, *Electrochimica Acta*, **282**, 448 (2018).
54. L.-C. Weng, A. T. Bell, and A. Z. Weber, *Physical Chemistry Chemical Physics*, **20**, 16973 (2018).
55. C. Georgopoulou, S. Jain, A. Agarwal, E. Rode, G. Dimopoulos, N. Sridhar, and N. Kakalis, *Computers & Chemical Engineering*, **93**, 160 (2016).
56. C. Delacourt and J. Newman, *Journal of The Electrochemical Society*, **157**, B1911 (2010).
57. M. Ni, *International Journal of Hydrogen Energy*, **37**, 6389 (2012).
58. M. Ni, *Journal of Power Sources*, **202**, 209 (2012).
59. Y. Xie and X. Xue, *Solid State Ionics*, **224**, 64 (2012).
60. Y. Luo, Y. Shi, W. Li, and N. Cai, *Energy*, **70**, 420 (2014).
61. C. Delacourt, P. L. Ridgway, and J. Newman, *Journal of The Electrochemical Society*, **157**, B1902 (2010).
62. C. Oloman and H. Li, *ChemSusChem*, **1**, 385 (2008).
63. H. Li and C. Oloman, *Journal of Applied Electrochemistry*, **37**, 1107 (2007).
64. N. Gupta, M. Gattrell, and B. MacDougall, *Journal of Applied Electrochemistry*, **36**, 161 (2006).
65. F. Proietto, A. Galia, and O. Scialdone, *ChemElectroChem*,**0** (2018).
66. T. Burdyny, P. J. Graham, Y. Pang, C.-T. Dinh, M. Liu, E. H. Sargent, and D. Sinton, *ACS Sustainable Chemistry & Engineering*, **5**, 4031 (2017).
67. M. Lindstrom and B. Wetton, *Heat and Mass Transfer*, **53**, 205 (2017).
68. Z. Duan, R. Sun, C. Zhu, and I. M. Chou, *Marine Chemistry*, **98**, 131 (2006).
69. H. Zhong, K. Fujii, Y. Nakano, and F. Jin, *The Journal of Physical Chemistry C*, **119**, 55 (2015).
70. Y. Tang, X. Bian, Z. Du, and C. Wang, *Fluid Phase Equilibria*, **386**, 56 (2015).
71. J. Qiao, Y. Liu, and J. Zhang, *Electrochemical Reduction of Carbon Dioxide: Fundamentals and Technologies*, CRC Press (2016).
72. Q. Dong, S. Santhanagopalan, and R. E. White, *Journal of The Electrochemical Society*, **154**, A816 (2007).
73. W. Lv, S. Liu, R. Zhang, W. Wang, Z. Wang, L. Wang, and W. Wang, *Journal of Materials Science*, **53**, 4939 (2018).
74. D. T. Whipple and P. J. A. Kenis, *The Journal of Physical Chemistry Letters*, **1**, 3451 (2010).
75. Conductance Data For Commonly Used Chemicals, in, Emerson Process Management (2010).
76. X. Li, C. Peng, J. P. Crawshaw, G. C. Maitland, and J. P. M. Trusler, *Fluid Phase Equilibria*, **458**, 253 (2018).
77. J. Kubisztal and A. Budniok, *International Journal of Hydrogen Energy*, **33**, 4488 (2008).
78. X. Han, Z. Yu, J. Qu, T. Qi, W. Guo, and G. Zhang, *Journal of Chemical & Engineering Data*, **56**, 1213 (2011).